

## **Bromodomain inhibition reveals FGF15/19 as a target of epigenetic regulation and metabolic control**

Chisayo Kozuka<sup>1,2,3</sup>, Vissarion Efthymiou<sup>1,2</sup>, Vicencia M. Sales<sup>1,2</sup>, Liyuan Zhou<sup>1,4</sup>, Soravis Osataphan<sup>1,2</sup>, Yixing Yuchi<sup>1,2</sup>, Jeremy Chimene-Weiss<sup>1</sup>, Christopher Mulla<sup>1,2</sup>, Elvira Isganaitis<sup>1,2</sup>, Jessica Desmond<sup>1</sup>, Suzuka Sanechika<sup>1</sup>, Joji Kusuyama<sup>1,2</sup>, Laurie Goodyear<sup>1,2</sup>, Xu Shi<sup>2,4</sup>, Robert E. Gerszten<sup>2,4</sup>, Cristina Aguayo-Mazzucato<sup>1,2</sup>, Priscila Carapeto<sup>1,2</sup>, Silvania DaSilva Teixeira<sup>6</sup>, Darleen Sandoval<sup>6</sup>, Direna Alonso-Curbelo<sup>7</sup>, Lei Wu<sup>2,5</sup>, Jun Qi<sup>2,5</sup>, and Mary-Elizabeth Patti<sup>1,2,\*</sup>

### **Supplemental material**

#### ***Hyperinsulinemic-euglycemic clamp***

Hyperinsulinemic-euglycemic clamp was conducted in conscious mice as previously described (1). Briefly, following basal assessment, a primed, continuous infusion (150 mU/kg body weight bolus, then 1.25 mU/kg/min) of human insulin was initiated. At the end of the clamp, a bolus of <sup>14</sup>C deoxyglucose was administered prior to sacrifice and tissue dissection.

#### ***Metabolomics analysis***

Plasma and liver samples obtained at sacrifice (day16) were used for analysis of plasma and liver metabolites, using liquid chromatography-mass spectrometry (LC/MS) to determine metabolites, lipid class, and specific lipid content (2). Missing data were imputed with half of the minimum intensity of the metabolite, and the imputed data were quantile normalized and log<sub>2</sub>-transformed.

### ***Pancreatic islet isolation and glucose-stimulated insulin secretion***

Pancreatic islets were isolated as previously described (3). For insulin secretion assay, islets were isolated from 5 male C57BL/6 mice and cultured for 72 hours in RPMI-1640 medium (ThermoFisher Scientific) with or without JQ-1 (80 or 250 nM). Insulin secretion was measured by incubation in 2.9 mM or 20.2 mM glucose in Krebs-Ringer bicarbonate buffer.

### ***Primary hepatocyte isolation and measurement of glucose production***

Primary hepatocytes were isolated from C57BL/6 mice after liver perfusion with collagenase and seeded  $1 \times 10^5$  cells/ml into collagen coated plates containing DMEM (ThermoFisher Scientific). The media were changed after 4 hours and glucose production was measured the following day as previously described (4). Briefly, after 6 h serum starvation with or without JQ-1 and FGF19, cells were cultured in glucose and phenol red-free DMEM with or without insulin (10, 100 nM), JQ-1 (250 nM) and FGF19 (100 ng/ml) for 5 h. Medium glucose concentrations were measured with the Glucose (HK) Assay Kit (Sigma).

### **Supplemental Reference**

1. Kim JK: Hyperinsulinemic-euglycemic clamp to assess insulin sensitivity in vivo. *Methods Mol Biol* 2009;560:221-238
2. Roberts LD, Souza AL, Gerszten RE, Clish CB: Targeted metabolomics. *Curr Protoc Mol Biol* 2012;Chapter 30:Unit 30 32 31-24
3. Aguayo-Mazzucato C, Andle J, Lee TB, Jr., Midha A, Talemal L, Chipashvili V, Hollister-Lock J, van Deursen J, Weir G, Bonner-Weir S: Acceleration of beta Cell Aging Determines Diabetes and Senolysis Improves Disease Outcomes. *Cell Metab* 2019;30:129-142 e124
4. Matsumoto M, Sakai M: Glucose Production Assay in Primary Mouse Hepatocytes. *Bio-protocol* 2012;2:e284

**Supplemental Table 1. Transcriptome pathway analysis of liver in JQ1-treated mice**

**Supplemental Table 2. Primer sequences**

**Mouse**

Gene	Forward Sequence	Reverse Sequence
<i>Rpl13a</i>	CTGCTCTCAAGGTTGTTCCGGCT	CCTTCCGTTTCTCCTCCAGAGT
<i>Slc10a2</i> (ASBT)	GTCTGTCCCCCAAATGCAACT	CACCCCATAGAAAACATCACCA
<i>Gpbar1</i> (TGR5)	TGCTTCTTCCTAAGCCTACTACT	CTGATGGTTCCGGCTCCATAG
<i>Nr1h4</i> (FXR)	CTGGCATCTATGAACTCAGGC	CCATTCGCGGCTTCTTTGG
<i>Rxra</i>	ATGGACACCAAACATTTCTCTGC	CCAGTGGAGAGCCGATTCC
<i>Fgf15</i>	ACGTCCTTGATGGCAATCG	GAGGACCAAAACGAACGAAATT
<i>Nr0b2</i> (SHP)	AGGATGCTGTGACCTTCGAG	CAGCTCAAGGCTCCAGAAAGA
<i>Slc51a</i> (OST $\alpha$ )	ATGCATCTGGGTGAACAGAA	GAGTAGGGAGGTGAGCAAGC
<i>Slc51b</i> (OST $\beta$ )	GACCACAGTGCAGAGAAAGC	CTTGTCATCACCACCAGGAC
<i>Pck1</i> (PEPCK)	CTAACTTGCCATGATGAACC	CTTCACTGAGGTGCCAGGAG
<i>G6pc</i>	CTTTGACTCTCTGAAGCCCC	GGGCTAGGCAGTATGGGATA
<i>Acc</i>	CCTGAAGACCTTAAAGCCAATGC	CCAGCCCACACTGCTTGTA
<i>Fasn</i>	GCCCCGGGTAGCTCTGGGTGTA	TGCTCCCAGCTGCAGGC
<i>Ppara</i>	CTTCCCAAAGCTCCTTCAAAAA	CTGCGCATGCTCCGTG
<i>Cpt1a</i>	GCACTGCAGCTCGCACATTACAA	CTCAGACAGTACCTCCTTCAGGAA
<i>Srebp2</i>	GAACTTTTCTTAACGTGGGCCT	GAGCATGTCTTCGATGTCGTTCA
<i>Hmgcs1</i>	AACTGGTGCAGAAATCTCTAGC	GGTTGAATAGCTCAGAACTAGCC
<i>Hmgcr</i>	AGCTTGCCCGAATTGTATGTG	TCTGTTGTGAACCATGTGACTTC
<i>Nr1h3</i> (LXR)	AGGAGTGTCGACTTCGCAAA	CTCTTCTTGCCGCTTCAGTTT
<i>Cyp7a1</i>	GAACCTCCTTTGGACAACGGG	GGAGTTTGTGATGAAGTGGACAT
<i>Cyp8b1</i>	TGTCTACTCCCTACTGGGGC	GAGAGCCACCTTATCTCCGC
<i>Fgfr1c</i>	TGTTTGACCGGATCTACACACA	CTCCCACAAGAGCACTCCAA
<i>Fgfr2</i>	TCGCATTGGAGGCTATAAGG	CGGGACCACACTTTCCATAA
<i>Fgfr3</i>	GCCCCGAGCGAATGGATAAG	GGATGCTGCCAACTTGTTCT
<i>Fgfr4</i>	CGCCAGCCTGTCACTATACAAA	CCAGAGGACCTCGACTCCAA
<i>Klb</i>	TGTTCTGCTGCGAGCTGTTAC	TACCGGACTCACGTACTGTTT
<i>Krt20</i>	CCTGCGAATTGACAATGCTA	CCTTGGAGATCAGCTTCCAC
<i>Hnf1a</i>	GACCTGACCGAGTTGCCTAAT	CCGGCTCTTTCAGAATGGGT
<i>ChgA</i>	ATCCTCTCTATCCTGCGACAC	GGGCTCTGGTTCTCAAACACT
<i>Muc2</i>	AACGATGCCTACACCAAGGTC	ACTGAACTGTATGCCTTCCTCA
<i>Lgr5</i>	CCTACTCGAAGACTTACCCAGT	GCATTGGGGTGAATGATAGCA

<i>Reg4</i>	CTGGAATCCCAGGACAAAGAGTG	CTGGAGGCCTCCTCAATGTTTGC
<i>Ctnnb1</i> ( $\beta$ -catenin)	GCGGCCGCGAGGTACCTGAA	GCAGCTTTTCTGTCCGGCTCCA
<i>Gcg</i>	AGGGACCTTTACCAGTGATGT	GCGAATGGCGACTTCTTCTGGGAA
<i>Pyy</i>	ACGGTCGCAATGCTGCTAAT	GACATCTCTTTTCCATACCGCT
<i>Crp4</i>	AAGAGACTAAACTGAGGAGCAGC	CGGCGGGGGCAGCAGTA

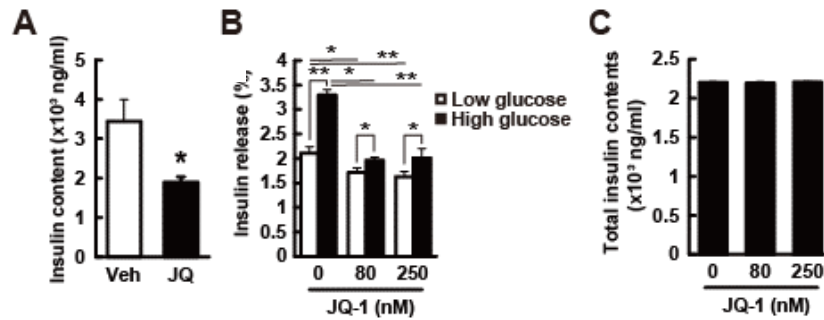
#### Human

Human Gene	Forward Sequence	Reverse Sequence
<i>BRD4</i>	CATGGACATGAGCACAATCA	TCATGGTCAGGAGGGTTGTA
<i>MYC</i>	GGCTCCTGGCAAAGGTCA	CTGCGTAGTTGTGCTGATGT
<i>FGF19</i>	CGGAGGAAGACTGTGCTTTTCG	CTCGGATCGGTACACATTGTAG
<i>NR0B2</i> (SHP)	ATCCTCTTCAACCCCGATGTG	ACTTCACACAGCACCCAGTG

#### ChIP-PCR

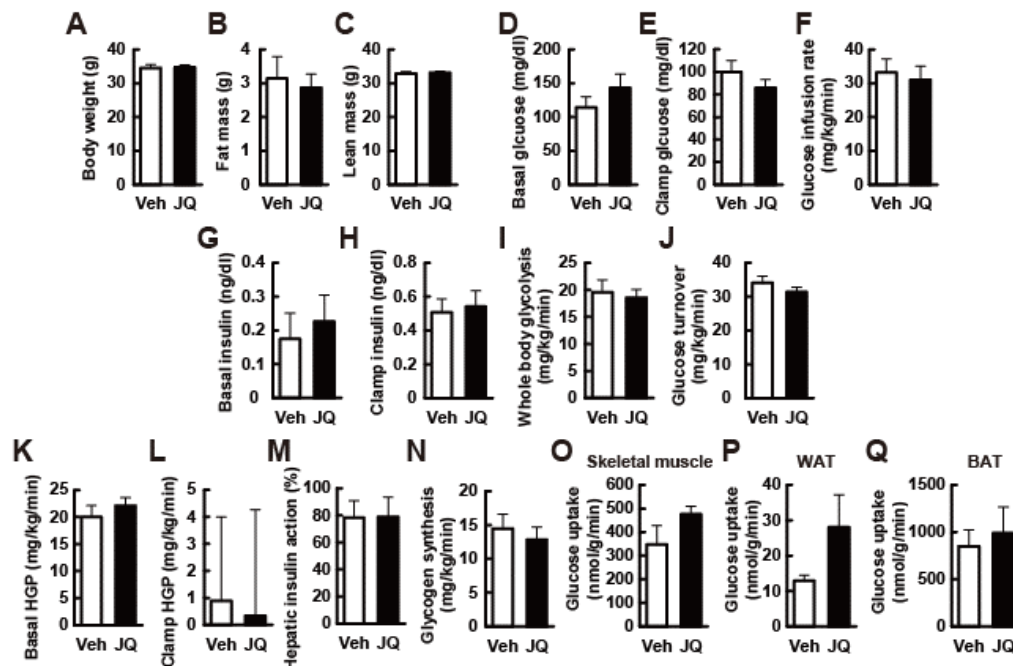
ChIP-PCR primers	Forward Sequence	Reverse Sequence
FGF19-1	GCTGGGACAAAGCATCGGA	TCCCAAAGGACAAGCCAAGTAA
FGF19-2	GTCCCGCTGTTACAAAGGA	CCACCCCAGAAAGGATGCAG
FGF19-3	GTGCGGTCCGTCCACAA	TTTTGGCACCTGGACGTTAG
SHP	TGGCTGGTGCTCATGGTTAG	TAAATAGCACCCACAGCGCA

**Supplemental Figure 1. JQ-1 decreases insulin content in islets isolated from mice treated in vivo, and reduces glucose stimulated insulin secretion after ex vivo incubation with JQ1.**



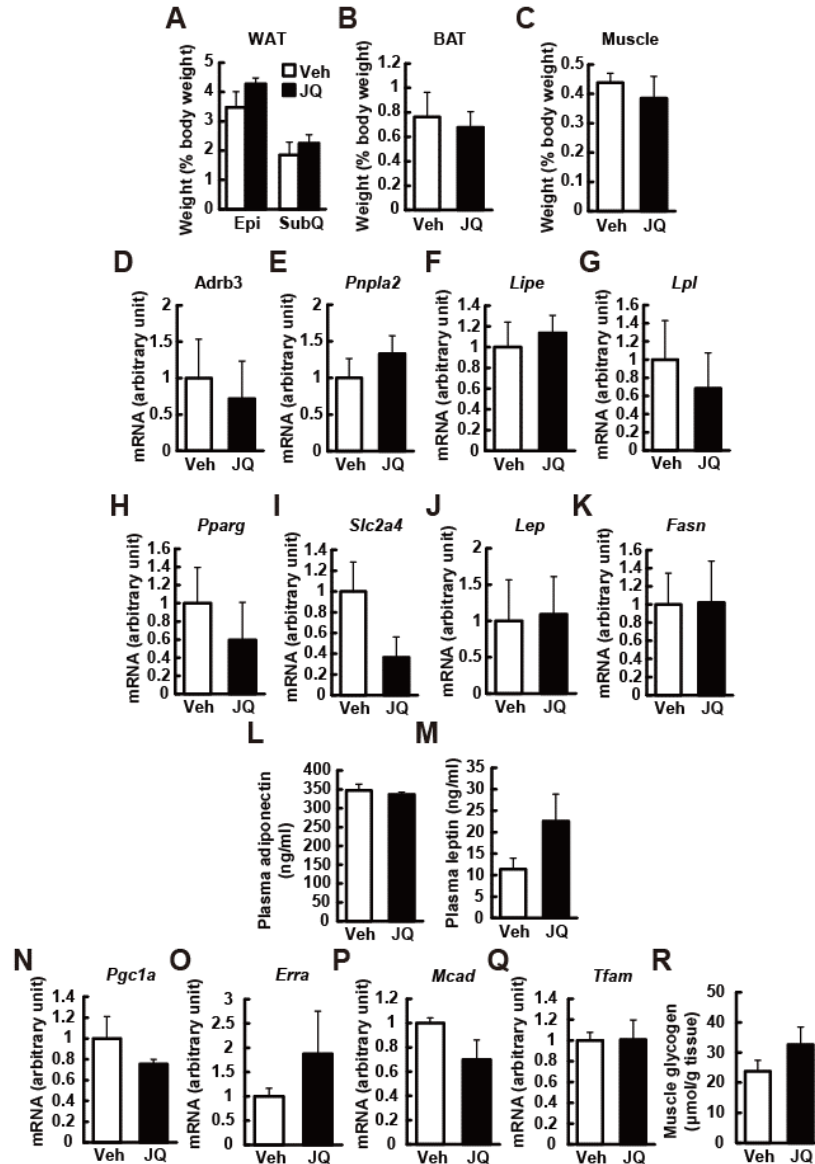
(A) Islet insulin content in pancreatic islets of JQ-1-treated mice. (B,C) Islets from 5 male C57BL/6 mice were divided into 3 groups: vehicle (Veh), JQ-1 at 80 nM and 250 nM. (B) Glucose-stimulated insulin secretion (GSIS) under low (2.9 mM) and high (20.2 mM) glucose Krebs-Ringer solutions (after 1h incubation). (C) Total insulin content. Islets of each group were isolated in triplicate. 20 islets per sample; 3 samples per animal. Data are expressed as means  $\pm$  SEM.

**Supplemental Figure 2. JQ-1 has no effect on systemic or tissue insulin sensitivity.**



Hyperinsulinemic-euglycemic clamp experiments were performed to assess insulin sensitivity (1.25 mU/kg/min insulin dose) ( $n = 5-6$ ). **(A)** Body weight, **(B)** fat mass, and **(C)** lean mass. **(D)** Basal glucose, **(E)** clamp glucose, **(F)** glucose infusion rate, **(G)** basal insulin, **(H)** clamp insulin, **(I)** whole body glycolysis, and **(J)** glucose turnover, **(K)** basal hepatic glucose production (HGP), **(L)** clamp HGP, **(M)** hepatic insulin action, **(N)** glycogen synthesis. **(O-Q)** Glucose uptake in skeletal muscle **(O)**, white adipose tissue (WAT) **(P)**, and brown adipose tissue (BAT) **(Q)**. Data are expressed as means  $\pm$  SEM.

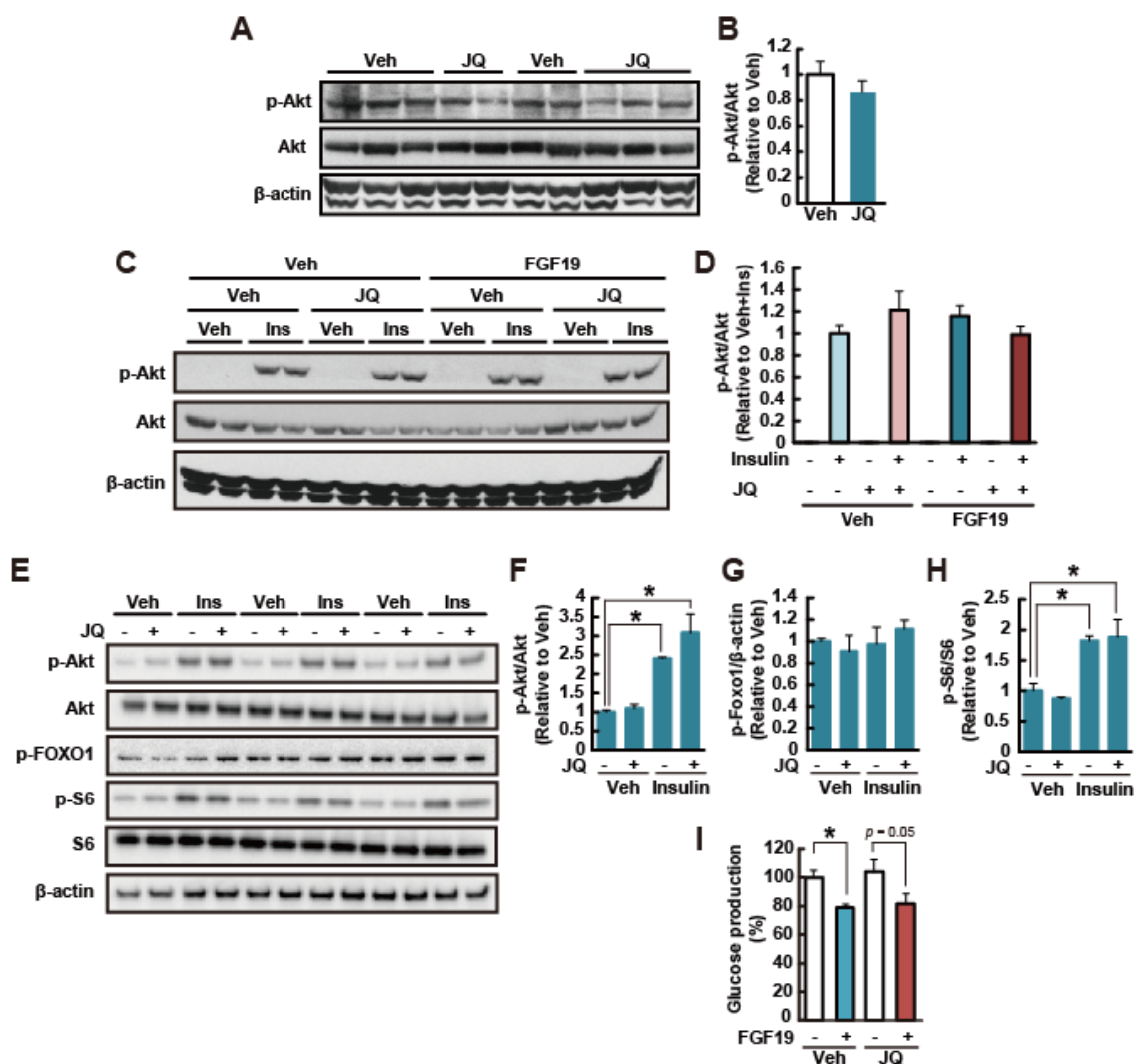
**Supplemental Figure 3. JQ-1 has minimal effect on adipose tissue and skeletal muscle.**



(A-C) Tissue weight of white adipose tissue (WAT) (A), brown adipose tissue (BAT) (B), and skeletal muscle (C) ( $n = 5-6$ ). Veh: Vehicle-treated mice, Epi: epididymal fat, SubQ: subcutaneous fat. (D-K) Epididymal adipose tissue expression of *Adrb3* ( $\beta 3$ -AdR) (D), *Pnpla2* (ATGL) (E), *Lipe* (HPL) (F), *Lpl* (G), *Pparg* (H), *Slc2a4* (GLUT4) (I), *Lep* (J), and *Fasn* (K) ( $n = 5-6$ ). (L, M) Plasma adiponectin (L) and leptin (M) levels ( $n = 5-6$ ). (N-Q) Gastrocnemius muscle expression of *PGC1 $\alpha$*  (N), *ERR $\alpha$*  (O), *MCAD* (P), and *TFAM* (Q) ( $n = 5-6$ ). Gene expression levels were normalized to *Rpl13*. (R) Glycogen contents in gastrocnemius muscle ( $n = 5-6$ ). Data are expressed as mean  $\pm$  SEM.

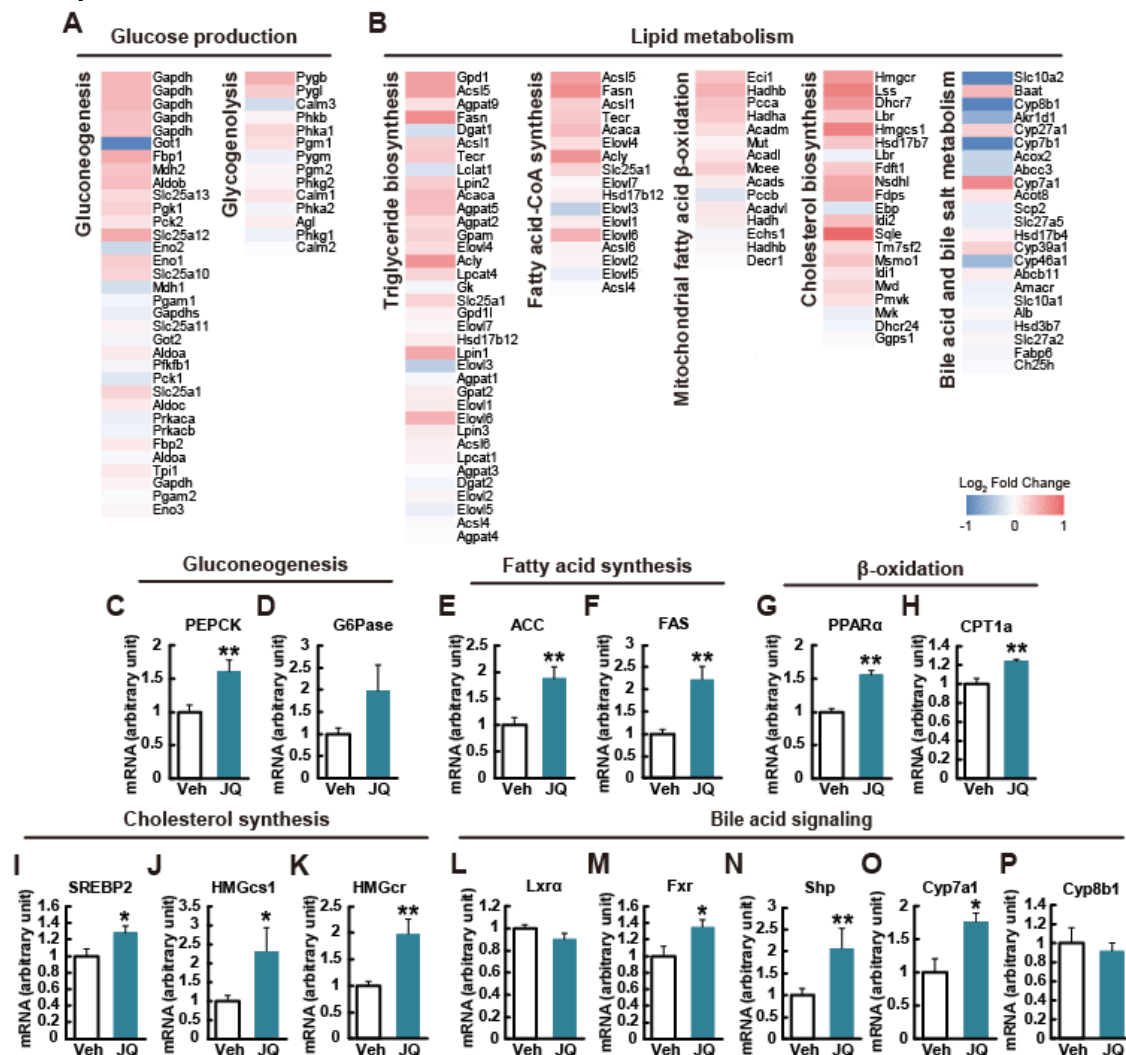


**Supplemental Figure 4. JQ-1 does not alter insulin signaling in liver extracts or either primary or cultured hepatocytes.**



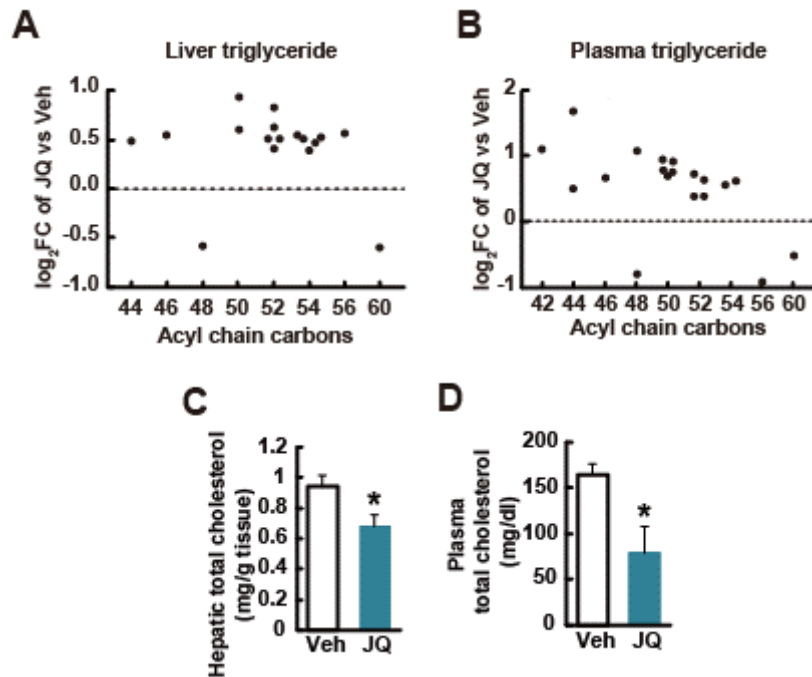
(**A, B**) Western blot analysis of total and phosphorylated Akt in liver lysates. β-actin is shown as a loading control ( $n = 5$ ). (**C-H**) Western blot analysis of total and phosphorylated Akt (**C-F**), FOXO1 (**E, G**), and S6 (**E, H**) in primary hepatocytes (**C, D**) and AML12 cells (**E-H**) ( $n = 3$ ). β-actin is shown as a loading control.  $*P < 0.05$ , vs. vehicle (Veh) or JQ-1-treated cells without insulin or FGF19. (**I**) Glucose production with or without FGF19 in primary hepatocytes ( $n = 3$ ).  $*P < 0.05$ , vs. vehicle (Veh) or JQ-1-treated cells without FGF19.

**Supplemental Figure 5. JQ-1 modulates expression of genes regulating glucose and lipid metabolism in the liver.**



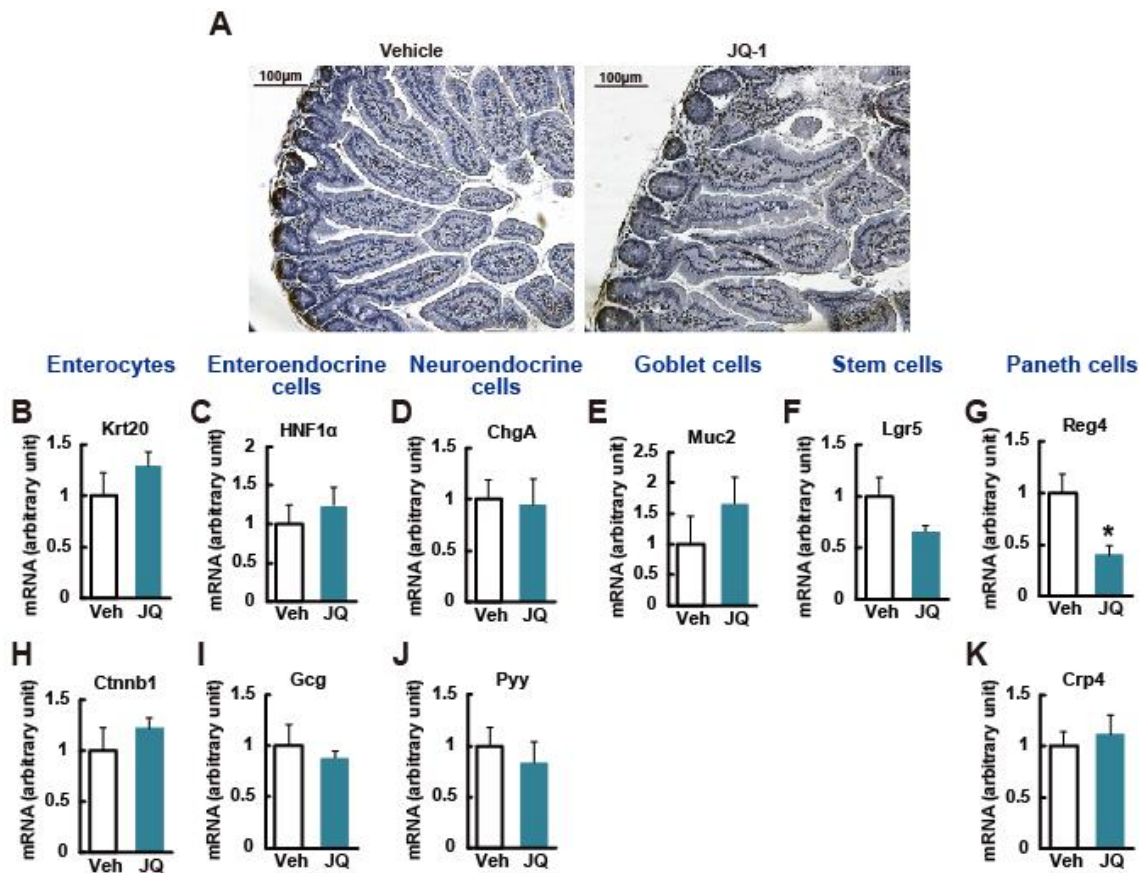
(A-B) Microarray analysis in the liver was performed in JQ-1-treated mice ( $n = 3$ ). Heatmaps represent log<sub>2</sub> fold changes in gene expression in pathways related to (A) glucose production, (B) lipid metabolism. Expression levels of genes related to (C, D) gluconeogenesis (*Pepck* (C) and *G6Pase* (D)), (E, F) fatty acid synthesis (*Acc* (E), and *Fasn* (F)), (G, H) β-oxidation (*Ppara* (G), and *Cpt1a* (H)), (I-K) cholesterol synthesis (*Srebp2* (I), *Hmgcs1* (J) and *Hmgcr* (K)) and (L-P) bile acid synthesis and signaling (*Nr1h3* (LXRα) (L), *Nr1h4* (FXR) (M), *Nr0b2* (SHP) (N), *Cyp7a1* (O), and *Cyp8b1* (P)) in the liver ( $n = 5-6$ ). The levels were normalized by those of *Rpl13*. \* $P < 0.05$ , \*\* $P < 0.01$ , vs. vehicle-treated mice (Veh). \* $P < 0.05$ , \*\* $P < 0.01$ , vs. vehicle-treated mice (Veh). Data are expressed as means  $\pm$  SEM.

**Supplemental Figure 6. JQ-1 modulates liver and plasma lipids.**



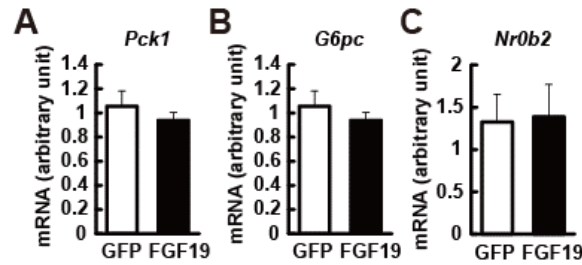
(**A, B**) Triglyceride species (FDR<0.25) are upregulated in JQ-1 liver (**A**) and plasma (**B**). X-axis indicates total acyl chain carbons, while Y-axis indicates log<sub>2</sub> fold change (JQ/vehicle). (**C, D**) Hepatic (**C**) and plasma (**D**) total cholesterol levels in JQ-1 treated mice ( $n = 5-6$ ). \* $P < 0.05$ , vs. vehicle-treated mice (Veh). Data are expressed as means  $\pm$  SEM.

**Supplemental Figure 7. JQ-1 decreases Reg4+ Paneth cells in the ileum.**



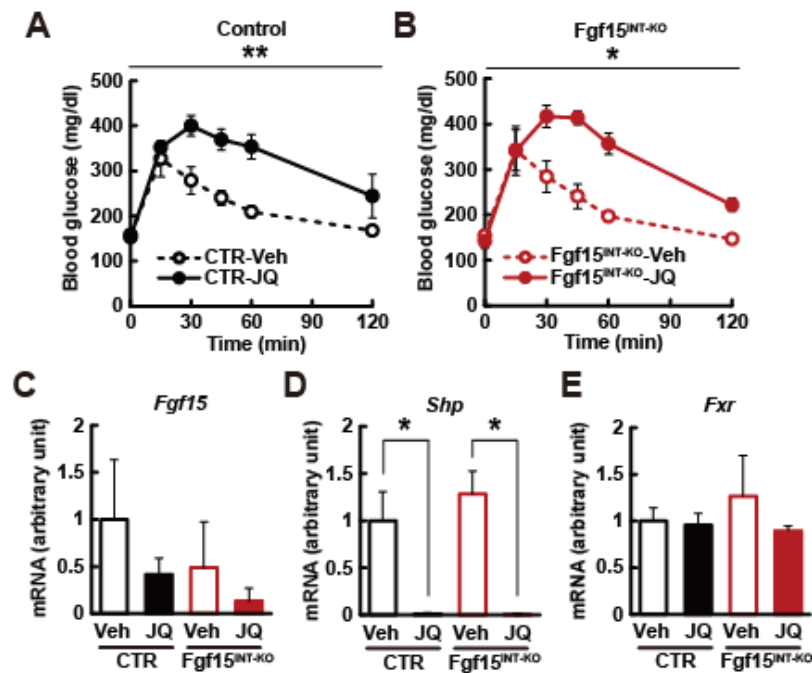
(A) Lysozyme staining of intestinal sections. Scale bar, 100  $\mu$ m. (B-K) Gene expression levels of cell type marker genes. Krt20 (B) and Ctnnb1 (H) are Enterocyte markers, HNF1 $\alpha$  (C) is an enteroendocrine cell marker, and the cells secrete Gcg (I). ChgA (D) is a neuroendocrine cell marker, and the cells secrete Pyy (J). Muc2 (E) and Lgr5 (F) are markers of goblet cell and stem cell, respectively. Reg4 (G) is a Paneth cell marker, and the cell secretes Crp4 (K). \* $P < 0.05$  vs. vehicle (Veh)-treated cells. Data are expressed as means  $\pm$  SEM.

**Supplemental Figure 8. Gluconeogenic gene expression levels were not changed by JQ-1 treatment in AAV-FGF19-treated mice.**



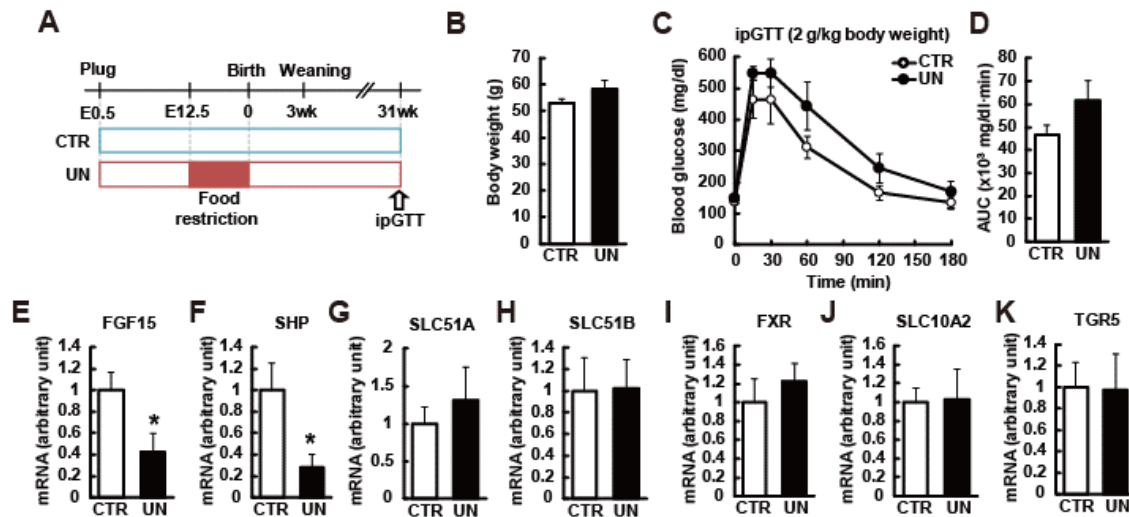
All animals were received JQ-1 treatment for 10 days. Gene expression levels of *Pepck* (*Pck1*) (A), *G6pc* (B), and *Shp* (*Nr0b2*) (C) in the liver ( $n = 5-6$ ). Gene expression levels were normalized by those of *36B4*. Data are expressed as means  $\pm$  SEM.

**Supplemental Figure 9. Glucose intolerance caused by JQ-1 treatment was seen in intestine-specific Fgf15 knockout ( $Fgf15^{INT-KO}$ ) mice.**



Control (CTR) and  $Fgf15^{INT-KO}$  mice were treated with JQ-1 (50 mg/kg/day ip) for 8 days. (**A, B**) Blood glucose levels during ipGTT in control (CTR) (**A**) and  $Fgf15^{INT-KO}$  (**B**) mice. (**C-E**) Gene expression levels of *Fgf15* (**C**), *Nr1h4* (*Fxr*) (**D**), *Nr0b2* (*Shp*) (**E**) in the liver ( $n = 3-8$ ). Gene expression levels were normalized by those of *36B4*. Data are expressed as means  $\pm$  SEM. \* $P < 0.05$ , \*\* $P < 0.01$ .

**Supplemental Figure 10. Expression of *Fgf15* and *Shp* is reduced in ileum in mice with developmental exposure to maternal undernutrition.**



(A) Experimental design. Control animals (CTR) and their mothers were housed with ad libitum access to chow diet. Food intake of mothers of undernutrition animals (UN) was restricted from day 12.5 until delivery by 50% compared with that consumed by mothers of CTR. After delivery, mothers and pups of both groups received chow ad libitum. (B) Body weight of CTR and UN at 31-week-old ( $n = 4-5$ ). (C, D) Blood glucose levels and area under the curve (AUC) during ipGTT ( $n = 4-5$ ). (E-K) Expression levels of genes related to bile acid signaling in ileum (*Fgf15* (E), *Nr0b2* (SHP) (F), *Slc51a* (OST $\alpha$ ) (G) and *Slc51b* (OST $\beta$ ) (H), *FXR* (I), *Slc10a2* (J), *Tgr5* (K)) ( $n = 4-5$ ). Expression levels were normalized by *Rpl13* expression. \* $P < 0.05$ , vs. CTR mice. Data are expressed as means  $\pm$  SEM.